

Interacting Particle Systems, Growth Models
and Random Matrices Workshop

Uniformly Random Lozenge Tilings of Polygons on the Triangular Lattice

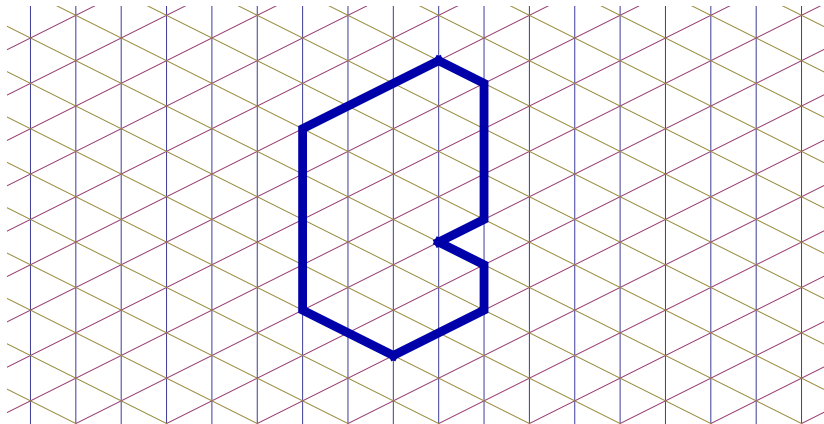
Leonid Petrov

Department of Mathematics, Northeastern University, Boston, MA, USA
and
Institute for Information Transmission Problems, Moscow, Russia

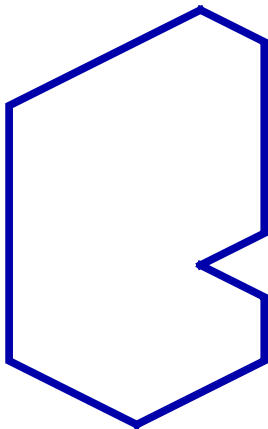
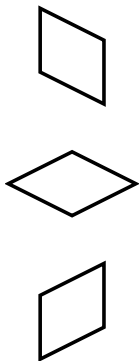
March 22, 2012

Model

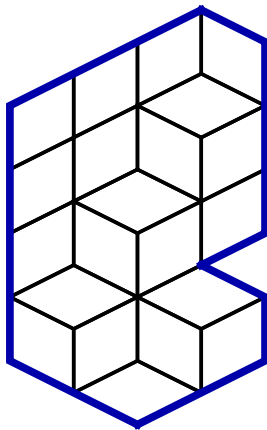
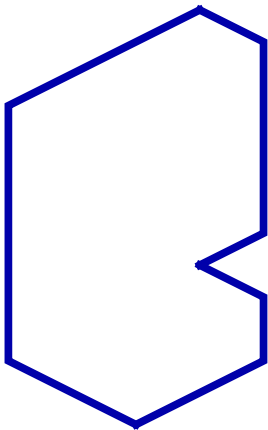
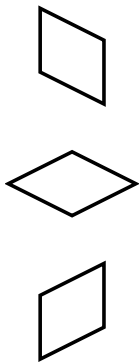
Polygon on the triangular lattice



Lozenge tilings of polygon



Lozenge tilings of polygon

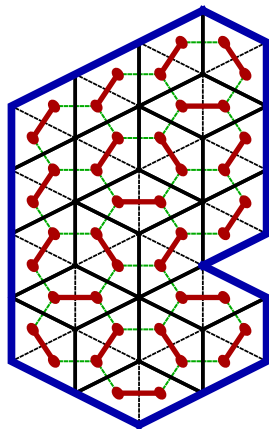
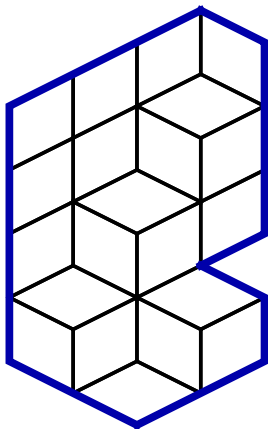


Remark

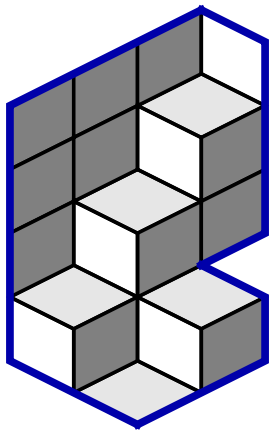
Lozenge tilings



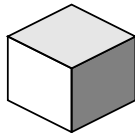
Dimer Coverings



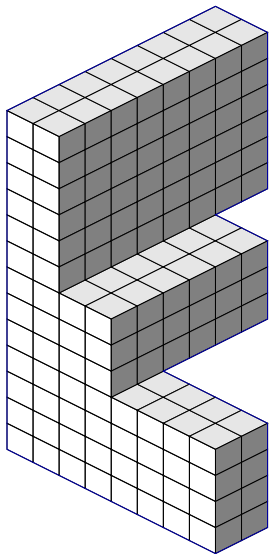
Tilings = 3D stepped surfaces



unit cube =

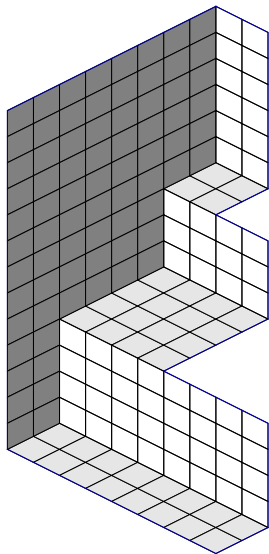


“full”

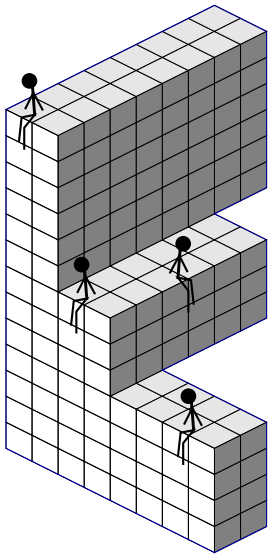


Remark:
and

“empty”

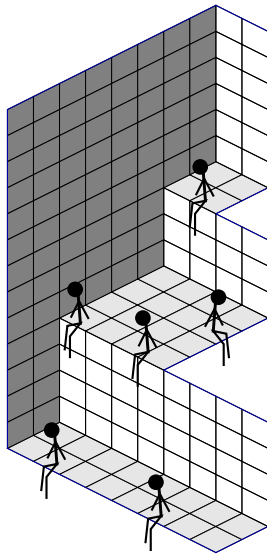


“full”



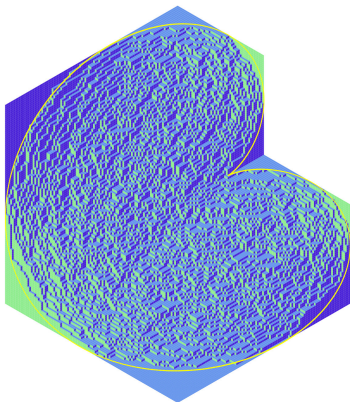
Remark:
and

“empty”

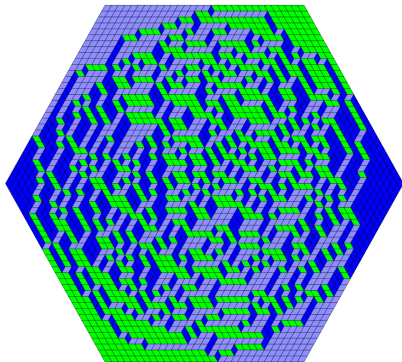


The model: uniformly random tilings

Fix a polygon \mathcal{P} and let the mesh $\rightarrow 0$.



[Kenyon-Okounkov '07]



Algorithm of [Borodin-Gorin '09]

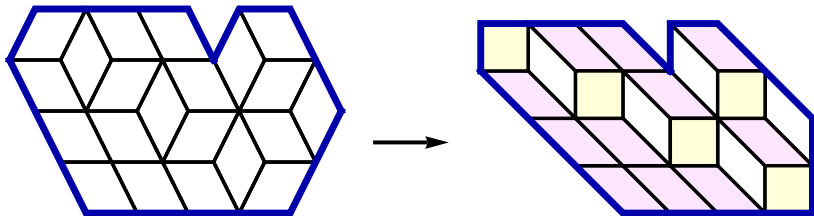
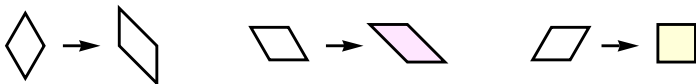
Limit shape and frozen boundary for general polygonal domains

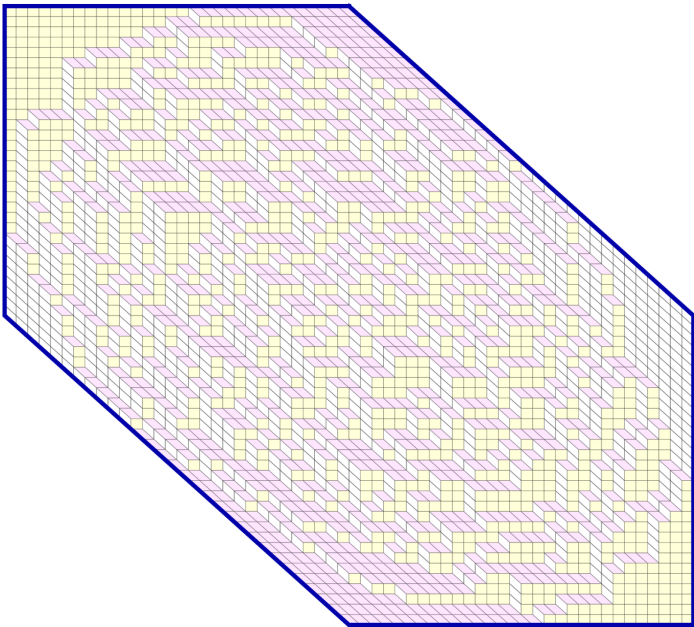
[Cohn–Larsen–Propp '98], [Cohn–Kenyon–Propp '01],
[Kenyon–Okounkov '07]

- (LLN) As the mesh goes to zero, random 3D stepped surfaces concentrate around a **deterministic limit shape surface**
- The limit shape develops **frozen facets**
- There is a connected **liquid region** where all three types of lozenges are present
- The limit shape surface and the separating **frozen boundary curve** are algebraic
- The frozen boundary is **tangent** to all sides of the polygon

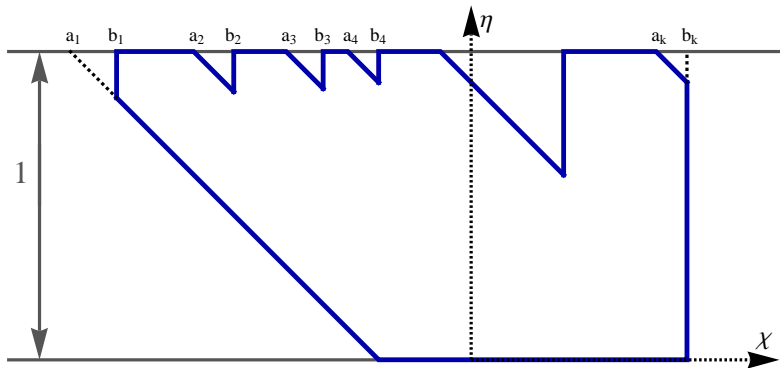
A class of polygons

Affine transform of lozenges





Class \mathfrak{P} of polygons in (x, η) plane



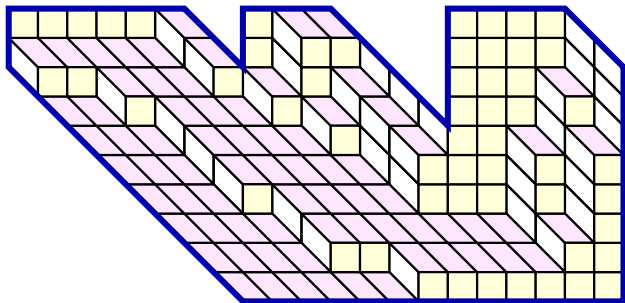
Polygon \mathcal{P} has $3k$ sides, $k = 2, 3, 4, \dots$

+ condition
$$\sum_{i=1}^k (b_i - a_i) = 1 \quad (a_i, b_i \text{ — fixed parameters})$$

($k = 2$ — hexagon with sides A, B, C, A, B, C)

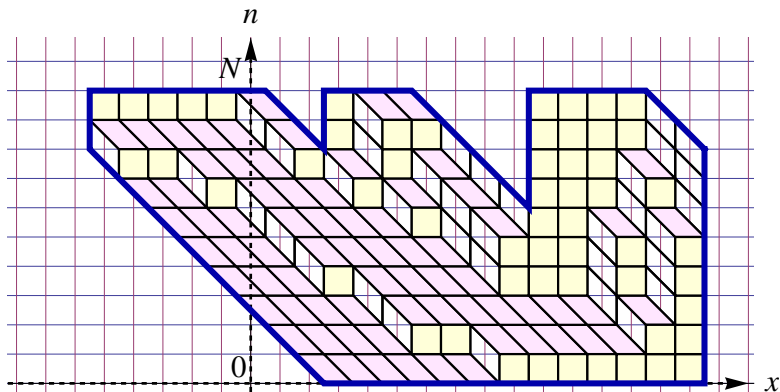
Patrice configurations and determinantal structure

Particle configurations



Take a tiling of a polygon \mathcal{P} in our class \mathfrak{P}

Particle configurations

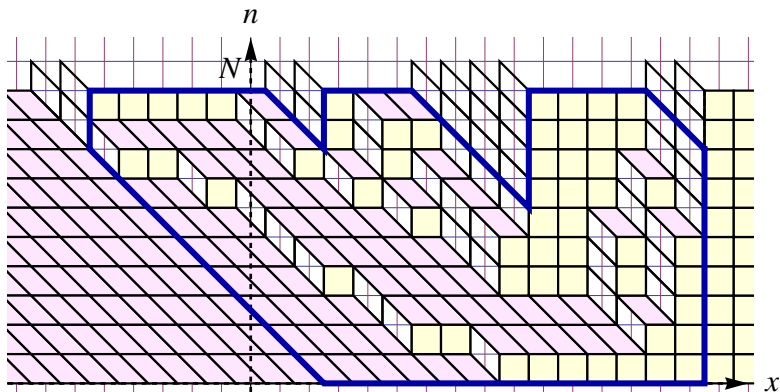


Let $N := \varepsilon^{-1}$ (where $\varepsilon =$ mesh of the lattice)

Introduce scaled *integer* coordinates (= blow the polygon)

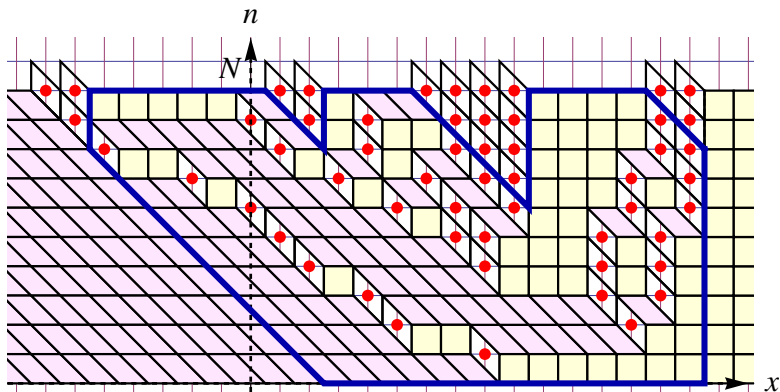
$$x = N\chi, \quad n = N\eta \quad (\text{so } n = 0, \dots, N)$$

Particle configurations



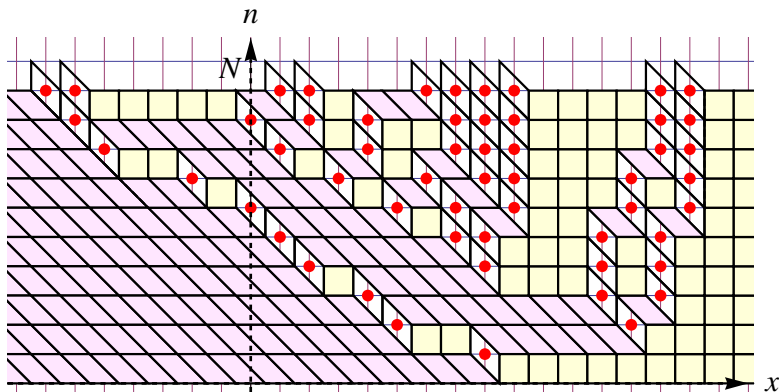
Trivially extend the tiling to the strip $0 \leq n \leq N$
with N small triangles on top

Particle configurations



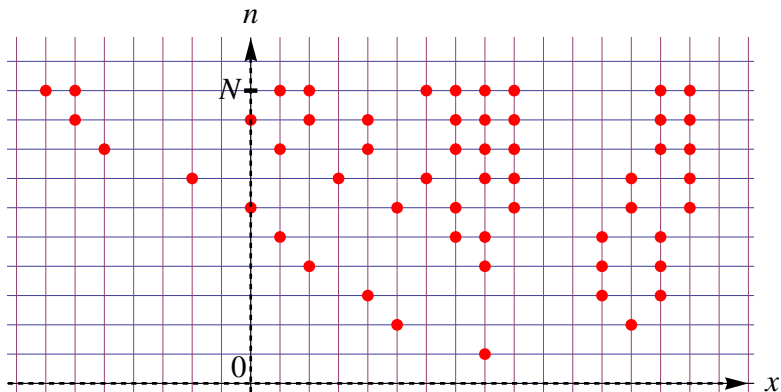
Place a particle in the center of every lozenge of type \blacklozenge

Particle configurations



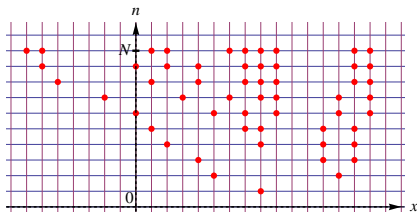
Erase the polygon...

Particle configurations



... and the lozenges!

(though one can always reconstruct everything back)



We get a **uniformly random integer (particle) array**

$$\{\mathbf{x}_j^m : m = 1, \dots, N; j = 1, \dots, m\} \in \mathbb{Z}^{N(N+1)/2}$$

satisfying **interlacing constraints**

$$\mathbf{x}_{j+1}^m < \mathbf{x}_j^{m-1} \leq \mathbf{x}_j^m \quad (\text{for all possible } m, j)$$

and with certain **fixed top (N -th) row**: $\mathbf{x}_N^N < \dots < \mathbf{x}_1^N$

(determined by N and parameters $\{a_i, b_i\}_{i=1}^k$ of the polygon).

Determinantal structure

Correlation functions

Fix some (pairwise distinct) positions $(x_1, n_1), \dots, (x_s, n_s)$,

$\rho_s(x_1, n_1; \dots; x_s, n_s) := \text{Prob}\{\text{there is a particle of random configuration } \{\mathbf{x}_j^m\} \text{ at position } (x_\ell, n_\ell), \ell = 1, \dots, s\}$

Determinantal correlation kernel

There is a function $K(x_1, n_1; x_2, n_2)$ (*correlation kernel*) s.t.

$$\rho_s(x_1, n_1; \dots; x_s, n_s) = \det[K(x_i, n_i; x_j, n_j)]_{i,j=1}^s$$

(for uniformly random tilings this follows, e.g., from Kasteleyn theory, cf. [Kenyon "Lectures on dimers" '09])

Problem:

there was no good explicit formula for the kernel $K(x_1, n_1; x_2, n_2)$ suitable for asymptotic analysis.

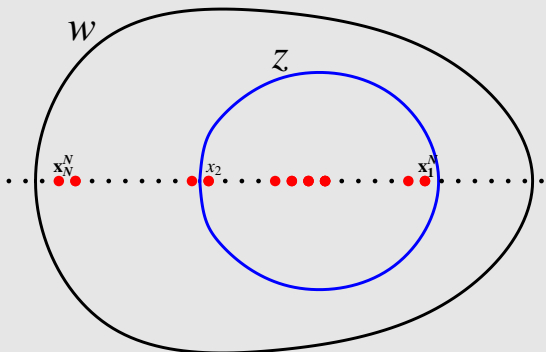
Theorem 1 [P. '12]. Explicit formula for the determinantal kernel of random interlacing integer arrays with the fixed top (N -th) row

$$\begin{aligned}
 K(x_1, n_1; x_2, n_2) &= -1_{n_2 < n_1} 1_{x_2 \leq x_1} \frac{(x_1 - x_2 + 1)_{n_1 - n_2 - 1}}{(n_1 - n_2 - 1)!} \\
 &+ \frac{(N - n_1)!}{(N - n_2 - 1)!} \frac{1}{(2\pi i)^2} \times \\
 &\times \oint_{\{w\}} \oint_{\{z\}} \frac{dz dw}{w - z} \cdot \frac{(z - x_2 + 1)_{N - n_2 - 1}}{(w - x_1)_{N - n_1 + 1}} \cdot \prod_{r=1}^N \frac{w - \mathbf{x}_r^N}{z - \mathbf{x}_r^N}
 \end{aligned}$$

where $1 \leq n_1 \leq N$, $1 \leq n_2 \leq N - 1$, and $x_1, x_2 \in \mathbb{Z}$, and $(a)_m := a(a + 1) \dots (a + m - 1)$

Theorem 1 [P. '12] (cont.). Contours of integration for K

- Both contours are counter-clockwise.
- $\{z\} \ni x_2, x_2 + 1, \dots, x_1^N, \quad \{z\} \not\ni x_2 - 1, x_2 - 2, \dots, x_N^N$
- $\{w\} \supset \{z\}, \quad \{w\} \ni x_1, x_1 - 1, \dots, x_1 - (N - n_1)$



reminder: integrand contains

$$\frac{(z - x_2 + 1)_{N-n_2-1}}{(w - x_1)_{N-n_1+1}} \prod_{r=1}^N \frac{w - x_r^N}{z - x_r^N}$$

Idea of proof of Theorem 1

Step 1. Pass to the q -deformation q^{vol} , vol = volume under the stepped surface

Step 2. Write the measure q^{vol} on interlacing arrays as a product of determinants

$$\text{Const} \cdot \det[\psi_i(\mathbf{x}_j^N)]_{i,j=1}^N \prod_{n=1}^N \det[\varphi_n(\mathbf{x}_i^{n-1}, \mathbf{x}_j^n)]_{i,j=1}^n$$

Main trick

Use a very special choice of ψ_i (related to the inverse Vandermonde matrix), which is why it all works

Idea of proof of Theorem 1.

Inverse Vandermonde matrix

Let V denote the $N \times N$ Vandermonde matrix $[(q^{x_i^N})^{N-j}]_{i,j=1}^N$.
Let V^{-1} be the inverse of that Vandermonde matrix.

Define the following functions in $x \in \mathbb{Z}$:

$$\psi_i(x) := \sum_{j=1}^N V_{ij}^{-1} \cdot 1(x = \mathbf{x}_j^N).$$

For $y_1 > \dots > y_N$:

$$\det[\psi_i(y_j)]_{i,j=1}^N = \frac{1(y_1 = \mathbf{x}_1^N) \dots 1(y_N = \mathbf{x}_N^N)}{\prod_{k < r} (q^{x_k^N} - q^{x_r^N})}$$

Idea of proof of Theorem 1.

Inverse Vandermonde matrix

Double contour integrals come from the following fact:

$$V_{ij}^{-1} = \frac{1}{(2\pi i)^2} \oint_{\{z\}} dz \oint_{\{w\}} \frac{dw}{w^{N+1-i}} \frac{1}{w-z} \prod_{r=1}^N \frac{w - q^{x_r^N}}{z - q^{x_r^N}}$$

The $\{z\}$ contour is around $q^{x_j^N}$, and the $\{w\}$ contour contains $\{z\}$ and is sufficiently big.

Idea of proof of Theorem 1

Step 3. Apply the Eynard-Mehta type formalism with varying number of particles [Borodin "Determin. P.P." '09]

The "Gram matrix" that one needs to invert is **diagonal!**

Step 4. Obtain the q -deformed correlation kernel

$$\begin{aligned} qK(x_1, n_1; x_2, n_2) &= -1_{n_2 < n_1} 1_{x_2 \leq x_1} q^{n_2(x_1 - x_2)} \frac{(q^{x_1 - x_2 + 1}; q)_{n_1 - n_2 - 1}}{(q; q)_{n_1 - n_2 - 1}} \\ &+ \frac{(q^{N-1}; q^{-1})_{N-n_1}}{(2\pi i)^2} \oint dz \oint \frac{dw}{w} \frac{q^{n_2(x_1 - x_2)} z^{n_2}}{w - z} \frac{(zq^{1-x_2+x_1}; q)_{N-n_2-1}}{(q; q)_{N-n_2-1}} \times \\ &\times {}_2\phi_1(q^{-1}, q^{n_1-1}; q^{N-1} \mid q^{-1}; w^{-1}) \prod_{r=1}^N \frac{w - q^{x_r^N - x_1}}{z - q^{x_r^N - x_1}}. \end{aligned}$$

Step 5. Pass to the limit $q \rightarrow 1$ (this kills ${}_2\phi_1$)



Connection to known kernels

The above kernel $K(x_1, n_1; x_2, n_2)$ generalizes some known kernels arising in the following models:

- ① Certain cases of the general Schur process
[Okounkov-Reshetikhin '03]
- ② Extremal characters of the infinite-dimensional unitary group \Rightarrow certain ensembles of random tilings of the entire upper half plane [Borodin-Kuan '08], [Borodin '10]
- ③ Eigenvalue minor process of random Hermitian $N \times N$ matrices with fixed level N eigenvalues \Rightarrow random continuous interlacing arrays of depth N [Metcalfe '11]

All these models can be obtained from tilings of polygons via suitable degenerations

Asymptotic analysis of the kernel

Write the kernel as

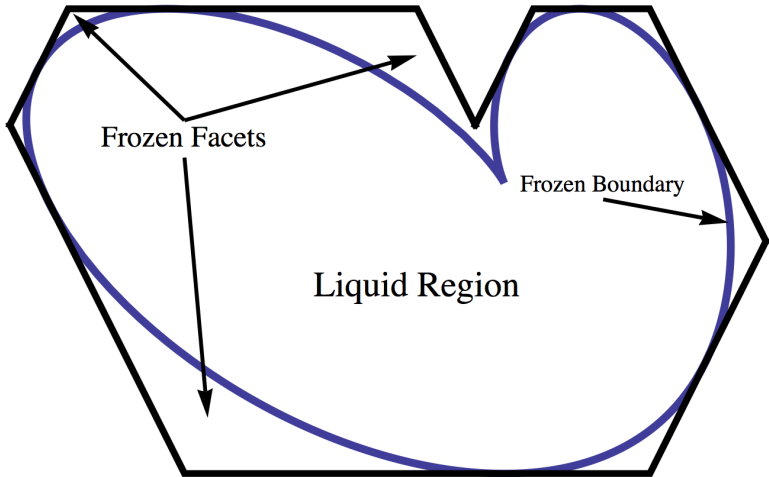
$$K(x_1, n_1; x_2, n_2) \sim \text{additional summand} \\ + \frac{1}{(2\pi i)^2} \oint \oint f(w, z) \frac{e^{N[S(w; \frac{x_1}{N}, \frac{n_1}{N}) - S(z; \frac{x_2}{N}, \frac{n_2}{N})]}}{w - z} dw dz$$

($f(w, z)$ — some “regular” part having a limit), where

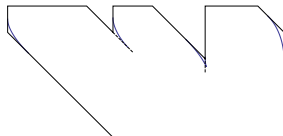
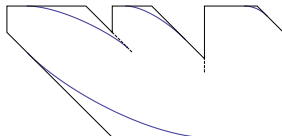
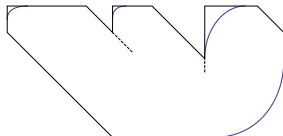
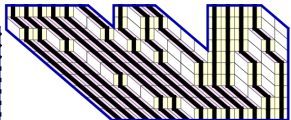
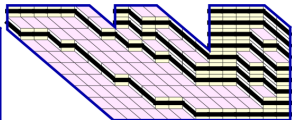
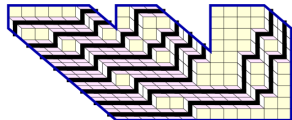
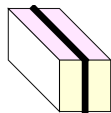
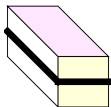
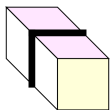
$$S(w; \chi, \eta) = (w - \chi) \ln(w - \chi) \\ - (w - \chi + 1 - \eta) \ln(w - \chi + 1 - \eta) + (1 - \eta) \ln(1 - \eta) \\ + \sum_{i=1}^k \left[(b_i - w) \ln(b_i - w) - (a_i - w) \ln(a_i - w) \right].$$

Then investigate critical points of the *action* $S(w; \chi, \eta)$ and transform the contours of integration [Okounkov "Symmetric functions and random partitions" '02]

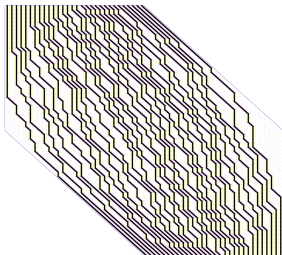
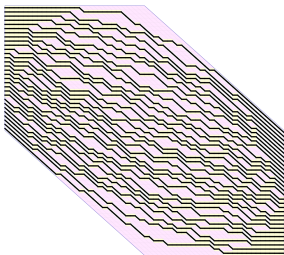
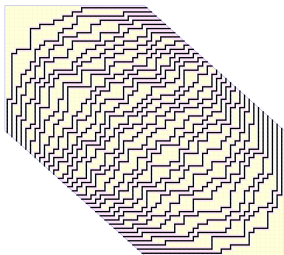
Asymptotic behavior of random tilings



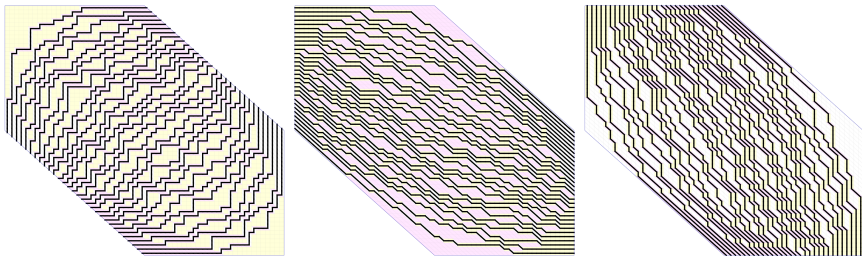
Local behavior at the edge: 3 directions of nonintersecting paths



Limit shape \Rightarrow outer paths of every type concentrate around the corresponding direction of the frozen boundary:



Limit shape \Rightarrow outer paths of every type concentrate around the corresponding direction of the frozen boundary:



Theorem 2 [P. '12]. Local behavior at the edge *for all polygons in the class \mathfrak{P}*

Fluctuations $O(\varepsilon^{1/3})$ in tangent and $O(\varepsilon^{2/3})$ in normal direction
($\varepsilon = \frac{1}{N}$ = mesh of the triangular lattice)

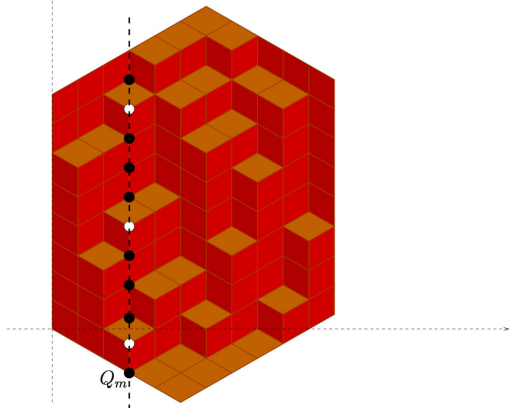
Thus scaled fluctuations are governed by the (space-time) Airy process at **not tangent nor turning** point $(\chi, \eta) \in$ **boundary**

Appearance of Airy-type asymptotics

- Edge asymptotics in many spatial models are governed by the Airy process (*universality*)
- First appearances:
random matrices (in particular, Tracy-Widom distribution F_2),
random partitions (in particular, the longest increasing subsequence)
— the static case
- Dynamical Airy process:
PNG droplet growth, [Prähofer–Spohn '02]
- Random tilings of infinite polygons:
[Okounkov-Reshetikhin '07]

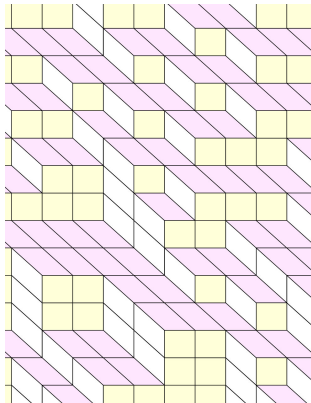
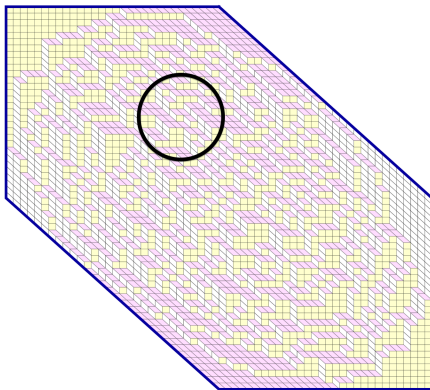
Finite polygons (our setting)

Hexagon case: [Baik-Kriecherbauer-McLaughlin-Miller '07], static case (in cross-sections of ensembles of nonintersecting paths), using orthogonal polynomials



Theorem 3 [P. '12]. Bulk local asymptotics *for all polygons in the class \mathfrak{P}*

Zooming around a point $(\chi, \eta) \in \mathcal{P}$, we asymptotically see a unique translation invariant ergodic Gibbs measure on tilings of the whole plane **with given proportions of lozenges** of all types [Sheffield '05], [Kenyon-Okounkov-Sheffield '06]

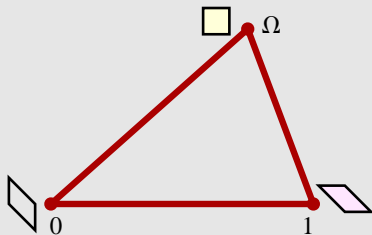


Theorem 3 [P. '12] (cont.). Proportions of lozenges

There exists a function $\Omega = \Omega(\chi, \eta): \mathcal{P} \rightarrow \mathbb{C}$, $\Im \Omega \geq 0$ (*complex slope*) such that asymptotic proportions of lozenges

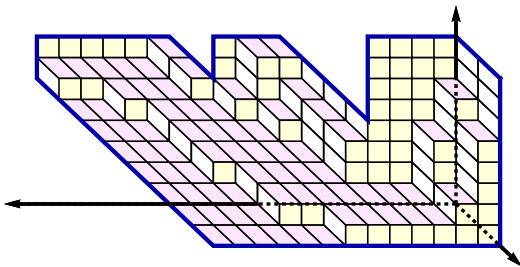
$$(p_{\swarrow}, p_{\square}, p_{\searrow}), \quad p_{\swarrow} + p_{\square} + p_{\searrow} = 1$$

(seen in a large box under the ergodic Gibbs measure) are the normalized angles of the triangle in the complex plane:



Predicting the limit shape from bulk local asymptotics

$(p_{\triangleleft}, p_{\square}, p_{\triangle})$ — normal vector to the limit shape surface in 3D coordinates like this:



Theorem 3 [P. '12] (cont.). Limit shape prediction

The limit shape prediction from local asymptotics coincides with the true limit shape of [Cohn–Kenyon–Propp '01], [Kenyon–Okounkov '07].

Bulk local asymptotics: previous results related to Theorem 3

- [Baik-Kriecherbauer-McLaughlin-Miller '07], [Gorin '08] — for uniformly random tilings of the hexagon (orth. poly)
- [Borodin-Gorin-Rains '10] — for more general measures on tilings of the hexagon (orth. poly)
- [Kenyon '08] — for uniform measures on tilings of general polygonal domains without frozen parts of the limit shape
- Many other random tiling models also show this local behavior (*universality*)

Theorem 4 [P. '12]. The complex slope $\Omega(\chi, \eta)$

The function $\Omega: \mathcal{P} \rightarrow \mathbb{C}$ satisfies the differential *complex Burgers equation* [Kenyon-Okounkov '07]

$$\Omega(\chi, \eta) \frac{\partial \Omega(\chi, \eta)}{\partial \chi} = -(1 - \Omega(\chi, \eta)) \frac{\partial \Omega(\chi, \eta)}{\partial \eta},$$

and the algebraic equation (it reduces to a degree k equation)

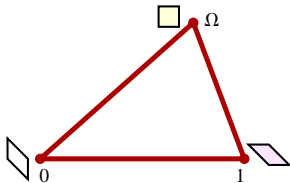
$$\begin{aligned} \Omega \cdot \prod_{i=1}^k ((a_i - \chi + 1 - \eta)\Omega - (a_i - \chi)) & \quad (1) \\ & = \prod_{i=1}^k ((b_i - \chi + 1 - \eta)\Omega - (b_i - \chi)). \end{aligned}$$

For (χ, η) in the liquid region, $\Omega(\chi, \eta)$ is the only solution of (1) in the upper half plane.

Parametrization of frozen boundary

(χ, η) approach the frozen boundary curve \Leftrightarrow

$\Omega(\chi, \eta)$ approaches the real line and becomes double root of the algebraic equation (1) thus yielding two equations on Ω , χ , and η .



We take slightly different real parameter for the frozen boundary curve:

$$t := \chi + \frac{(1 - \eta)\Omega}{1 - \Omega}.$$

Theorem 5 [P. '12]. Explicit rational parametrization of the frozen boundary curve $(\chi(t), \eta(t))$

$$\chi(t) = t + \frac{\Pi(t) - 1}{\Sigma(t)}; \quad \eta(t) = \frac{\Pi(t)(\Sigma(t) - \Pi(t) + 2) - 1}{\Pi(t)\Sigma(t)},$$

where

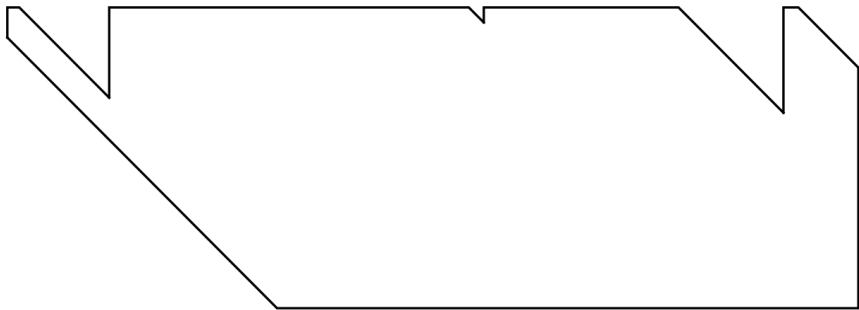
$$\Pi(t) := \prod_{i=1}^k \frac{t - b_i}{t - a_i}, \quad \Sigma(t) := \sum_{i=1}^k \left(\frac{1}{t - b_i} - \frac{1}{t - a_i} \right),$$

with parameter $-\infty \leq t < \infty$. As t increases, the frozen boundary is passed in the clockwise direction (so that the liquid region stays to the right).

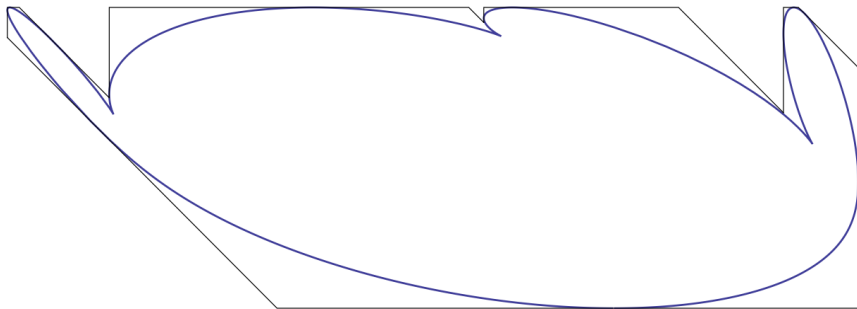
Tangent direction to the frozen boundary is given by

$$\frac{\dot{\chi}(t)}{\dot{\eta}(t)} = \frac{\Pi(t)}{1 - \Pi(t)}.$$

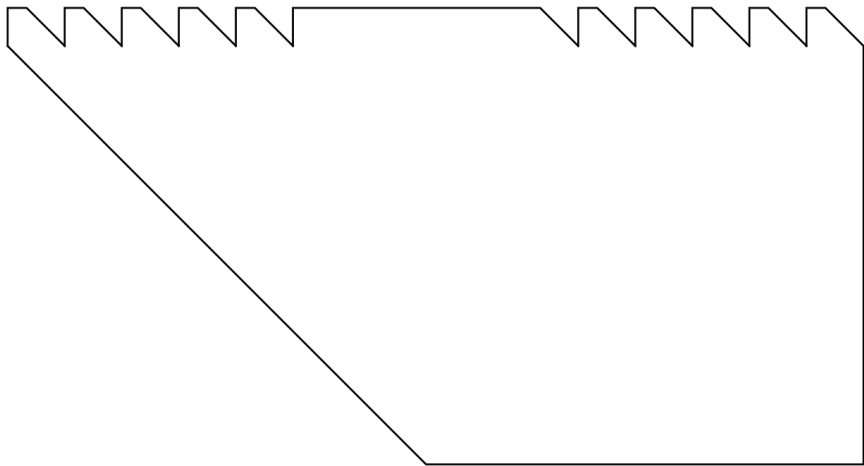
Frozen boundary examples



Frozen boundary examples



Frozen boundary examples



Frozen boundary examples

